BRAIN COMMUNICATIONS

REPORT

Biallelic NDUFA9 variants cause a progressive neurodevelopmental disorder with prominent dystonia and mitochondrial complex I deficiency

©Francesca Magrinelli, ¹ Lucie S. Taylor, ^{2,3} Sahar Sedighzadeh, ^{4,5} Dalila Moualek, ^{6,7} ©Mariasavina Severino, ⁸ ©Daniel N. Grba, ⁹ Charlotte L. Alston, ^{2,3} Michael Champion, ¹⁰ Ali Reza Tavasoli, ^{11,12} Karine Lascelles, ¹³ ©Vykuntaraju K. Gowda, ¹⁴ Varunvenkat M. Srinivasan, ¹⁴ Sahand Tehrani Fateh, ¹⁵ Mohammad Kordi-Tamandani, ¹⁶ Ali Khajeh, ¹⁷ Saeedeh Yaghoubi, ¹⁸ Natalia Dominik, ¹⁹ Meisam Babaei, ²⁰ Mohsen Javadzadeh, ²¹ Jamileh Rezazadeh Varaghchi, ²² Mohammad Miryounesi, ^{23,24} Ehsan Ghayoor Karimiani, ¹⁹ Meriem Tazir, ^{6,7} Lamia Ali Pacha, ^{6,7} Kailash P. Bhatia, ¹ Robert W. Taylor, ^{2,3} ©Henry Houlden ¹⁹ and ©Reza Maroofian ¹⁹

Biallelic *NDUFA9* variants have hitherto been associated with disease in four individuals. Hence, clinicogenetic features of *NDUFA9*-related disorder remain largely unexplored. To delineate the pheno-genotypic spectrum of *NDUFA9*-related disorder, we screened genetic databases worldwide and collected phenotypic data on individuals with biallelic *NDUFA9* variants, which were functionally investigated when possible. Eight new and four reported cases were identified. Neurodevelopmental delay followed by motor deterioration and seizures were the most common presenting features. Neurodevelopmental disorder was observed in 90% of cases surviving beyond the age of 4 months. Neurological deterioration always started in the first decade. Among ten affected surviving beyond early infancy, major clinical features included dystonia (100%), feeding difficulties/dysphagia/failure to thrive and pyramidal signs (80%), seizures and muscle weakness/atrophy (70%), and moderate-to-severe intellectual disability (60%). All showed basal ganglia MRI signal alterations, with atrophy (50%) and swelling (25%). Four individuals died by the age of 13 years. In addition to four known variants, we identified five new *NDUFA9* variants and pinpointed Arg360 (NP_004993.1) as a mutational hotspot. Protein modelling suggested that variants cause NADH:ubiquinone oxidoreductase subunit A9 (NDUFA9) misfolding and/or disruption of binding interfaces. Loss of fully assembled complex I with decreased steady-state NDUFA9 levels and/or complex I activity was documented in fibroblasts from three affected individuals. Our study strengthens the evidence that biallelic *NDUFA9* variants cause mitochondrial complex I deficiency presenting with a broad spectrum of progressive neurodevelopmental disorder, often accompanied by prominent dystonia, and a characteristic Leigh syndrome MRI pattern.

- 1 Department of Clinical and Movement Neurosciences, UCL Queen Square Institute of Neurology, University College London, London WC1N 3BG, United Kingdom
- 2 Mitochondrial Research Group, Translational and Clinical Research Institute, Faculty of Medical Sciences, Newcastle University, Newcastle upon Tyne NE2 4HH, United Kingdom
- 3 NHS Highly Specialised Service for Rare Mitochondrial Disorders, Newcastle upon Tyne Hospitals NHS Foundation Trust, Newcastle upon Tyne NE1 4LP, United Kingdom
- 4 Department of Biological Science, Faculty of Science, Shahid Chamran University of Ahvaz, Ahvaz 6135783151, Iran
- 5 Dr Shahrooei Laboratory, Tehran 1476693993, Iran

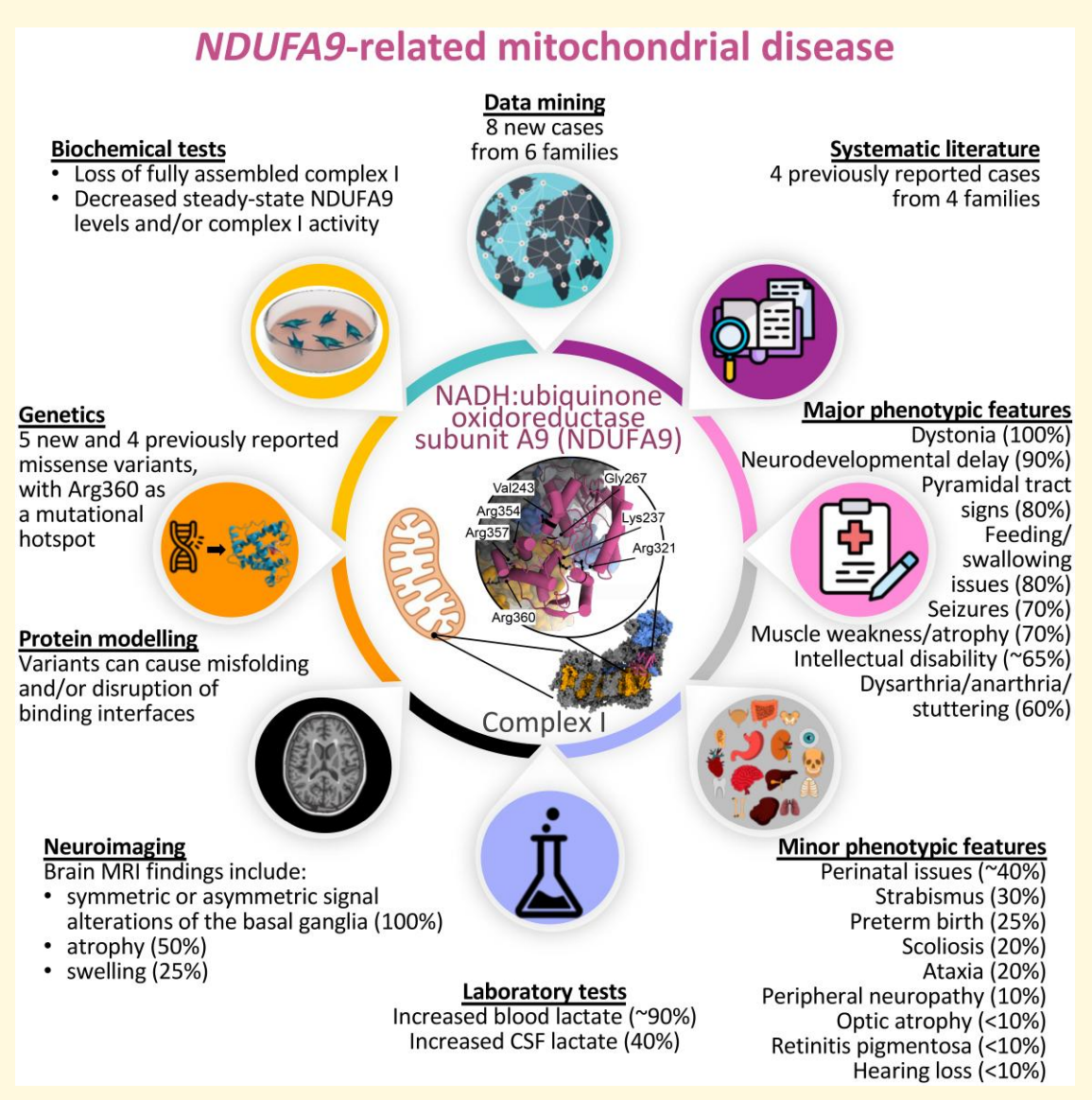
- 6 Service de Neurologie, CHU Mustapha Bacha, Alger 16000, Algeria
- 7 Université Benyoucef Benkhedda, Alger 16000, Algeria
- 8 Neuroradiology Unit, IRCCS Istituto Giannina Gaslini, Genova 16147, Italy
- 9 Medical Research Council Mitochondrial Biology Unit, University of Cambridge, Cambridge CB2 0XY, United Kingdom
- 10 Department of Paediatric Inherited Metabolic Disease, Evelina London Children's Hospital, Guy's and St Thomas' NHS Foundation Trust, London SE1 7EH, United Kingdom
- 11 Department of Neurology, Barrow Neurological Institute at Phoenix Children's Hospital, Phoenix, AZ 85016, USA
- 12 Myelin Disorders Clinic, Pediatric Neurology Division, Children's Medical Center, Tehran University of Medical Sciences, Tehran 1419733151, Iran
- 13 Children's Neuroscience Centre, Evelina London Children's Hospital, Guy's and St Thomas' NHS Trust, London SE1 7EH, United Kingdom
- 14 Department of Pediatric Neurology, Indira Gandhi Institute of Child Health, Near NIMHANS, Bengaluru, Karnataka 560029, India
- 15 School of Medicine, Tehran University of Medical Sciences (TUMS), Tehran 1416634793, Iran
- 16 Department of Biology, Faculty of Science, University of Sistan and Baluchestan, Zahedan 9816745785, Iran
- 17 Children and Adolescent Health Research Center, School of Medicine, Resistant Tuberculosis Institute, Zahedan University of Medical Sciences, Zahedan 9816743463, Iran
- 18 Department of Pediatrics, School of Medicine, Children and Adolescents Health Research Center, Research Institute of Cellular and Molecular Science in Infectious Diseases, Zahedan University of Medical Sciences, Zahedan 9816743463, Iran
- 19 Department of Neuromuscular Diseases, UCL Queen Square Institute of Neurology, London WC1N 3BG, United Kingdom
- 20 Department of Pediatrics, North Khorasan University of Medical Science, Bojnourd 9417694735, Iran
- 21 Department of Pediatric Neurology, Shahid Beheshti University of Medical Sciences, Tehran 1983969367, Iran
- 22 Hasti Genetic Counseling Center of Welfare Organization of Southern Khorasan, Birjand 9719866879, Iran
- 23 Center for Comprehensive Genetic Services, Shahid Beheshti University of Medical Sciences, Tehran 1985717413, Iran
- 24 Department of Medical Genetics, Faculty of Medicine, Shahid Beheshti University of Medical Sciences, Tehran 1985717443, Iran

Correspondence to: Francesca Magrinelli, MD, PhD Department of Clinical and Movement Neurosciences UCL Queen Square Institute of Neurology University College London, Queen Square London WC1N 3BG, United Kingdom

E-mail: f.magrinelli@ucl.ac.uk

Keywords: lactic acidosis; Leigh syndrome; mutational hotspot; seizures; spasticity

Graphical Abstract



Introduction

Complex I is the major multiprotein enzyme of the mitochondrial respiratory chain. Besides representing the main entry of electrons to the oxidative phosphorylation system (OXPHOS), it couples quinone reduction by NADH (reduced nicotinamide-adenine dinucleotide) to proton translocation across the inner mitochondrial membrane. The resulting electrochemical gradient ultimately drives protons back through the membrane via ATP synthase, which phosphorylates adenosine diphosphate (ADP) to ATP. Complex I consists of 14 catalytic core and 30 accessory subunits, 37 of which coded by nuclear DNA. Subunits are assembled in three functional modules: Q-module (ubiquinone reduction), N-module (NADH dehydrogenase) and P-module (proton translocation).

Encoded by the homonymous nuclear gene, NADH: ubiquinone oxidoreductase subunit A9 (NDUFA9) is a 39-kDa Q-module supernumerary subunit which is conserved in eukaryotes. NDUFA9 is synthetized in the cytosol and imported into mitochondria by an N-terminal presequence which is cleaved by matrix proteases. 6 In vitro, NDUFA9 is suggested to anchor complex I membrane and matrix arms by contributing to stability of a later stage assembly intermediate, as documented by gene knockout in human embryonic kidney 293T (HEK293T) cells. 1,6 Additionally, NDUFA9 is crucial for complex I function, as proven by the inability of the same cells to grow in galactose-containing medium.⁶ Given its location and membrane remodelling capacity, NDUFA9 has been implicated in recruiting the membrane-bound substrate ubiquinone-10 in complex I function.^{7,8} Finally, NDUFA9 has been implicated in regulating complex I in ischemia-reperfusion injury.

Leigh syndrome (LS) spectrum represents the most frequent presenting phenotype of childhood-onset mitochondrial disease, being causally linked to variants in over 110 genes across nuclear and mitochondrial genomes. ¹⁰ Biochemical defects in complex I cumulatively account for most cases of early-onset mitochondrial disease in humans. ¹¹⁻¹³ Nevertheless, biallelic *NDUFA9* variants have hitherto been linked to disease phenotypes in only four individuals, namely two cases of lethal infantile LS¹⁴⁻¹⁶ and two cases of childhood-onset generalized dystonia. ^{15,17}

We herein report eight new cases of *NDUFA9*-related mitochondrial disease from six unrelated families, harbouring five novel missense *NDUFA9* variants, three of which were investigated with functional studies of patient-derived fibroblasts.

Material and methods

Proband identification, phenotypic characterization and sampling

Individuals with homozygous or compound heterozygous NDUFA9 variants were identified by interrogating the University College London (UCL) Queen Square exome repository and next-generation sequencing datasets curated from national and international collaborators. Exome sequencing was performed on DNA extracted from whole blood across six different research and diagnostic laboratories, each employing slightly varying methodologies for sequencing and data analysis. We used Sanger sequencing to confirm NDUFA9 variants identified by next-generation sequencing in the probands and to perform segregation analysis on available genomic DNA from their family members, including both parents of seven affected individuals in Families 1-2-3-4-5 (12 individuals), two probands affected siblings (P2 in Families 1 and 2), and eight probands unaffected siblings in Families 1–2–3. Detailed clinical data were collected using a standardized proforma completed by referring clinicians for all affected individuals. Video recordings of neurological examinations were reviewed by movement disorder specialists (FM, KPB) when available. Neuroimaging was assessed by an experienced paediatric neuroradiologist (MS).

To facilitate functional studies, punch skin biopsies were obtained from proband F1-P1 (Fig. 1A), his affected brother (F1-P2), his unaffected mother (F1-P3), and proband F3-P1, from which dermal fibroblast cultures were established.

The study was conducted in accordance with the principles of the Declaration of Helsinki and received approval from local Ethics Committees. Written informed consent for video acquisition and genetic testing as well as for the publication of clinical, genetic data, and video recordings was obtained from the parents or guardians of the affected individuals.

Literature review

A systematic literature review was conducted using PubMed, Web of Science, and Google Scholar to identify published cases carrying biallelic *NDUFA9* variants with individual phenotypic information. The search term 'NDUFA9' was applied on 15 June 2025. Predetermined phenotypic and genotypic data were extracted from the identified studies and subsequently merged with information from our study cohort for comprehensive analysis.

Analysis and interpretation of NDUFA9 variants

Frequencies of newly and previously identified NDUFA9 variants in the healthy population were retrieved from gnomAD v4.1.0 and other open-source and private databases. Pathogenicity prediction of all NDUFA9 variants was assessed using multiple tools, including the Combined Annotation-Dependent Depletion (CADD; https://cadd.gs. washington.edu/snv), Deleterious Annotation of genetic variants using Neural Networks (DANN; accessed through Franklin, https://franklin.genoox.com), Polymorphism Phenotyping v2 (PolyPhen-2; http://genetics.bwh.harvard. edu/pph2/), Sorting Intolerant From Tolerant Databases for Genome (SIFT 4G; https://sift.bii.a-star.edu.sg/sift4g/public// Homo_sapiens/); MutationTaster (http://www.mutation taster.org/), and Rare Exome Variant Ensemble Learner (REVEL; https://sites.google.com/site/revelgenomics/), to predict the impact of variants on the protein structure and function. We examined the conservation of substituted amino acid residues using Genomic Evolutionary Rate Profiling (GERP; accessed through Franklin, https://franklin.genoox. com) and visual multiple sequence alignment of NDUFA9 across different species. Variants were finally classified according to the American College of Medical Genetics and Genomics (ACMG)/Association for Molecular Pathology (AMP) guidelines. 18

NDUFA9 protein modelling

The human complex I model (PDB 5XTD)¹⁹ was used as input for the University of California, San Francisco (UCSF) ChimeraX,²⁰ where the *rotamers* or *swapaa* functions were used to introduce NDUFA9 variants, with residues mutated to glycine using the latter. Rotamers of the highest prevalence in the ChimeraX library were chosen, with obvious clashing conformations not considered. The residues within 4 Å of the mutated residue were inspected for interactions. All images were generated in UCSF ChimeraX and organized in Affinity Designer 2.

Dermal fibroblast culture

Dermal fibroblasts were cultured in medium containing Dulbecco's Modified Eagle Medium (DMEM) supplemented with 1 mM pyruvate and 4.5 g/L glucose (ThermoFisher Scientific), 10% bovine foetal serum (ThermoFisher Scientific), 50 µg/mL uridine (Sigma), 1× non-essential amino acids (ThermoFisher Scientific), 1% penicillin/streptomycin (ThermoFisher Scientific) at 37°C in 5% CO₂.

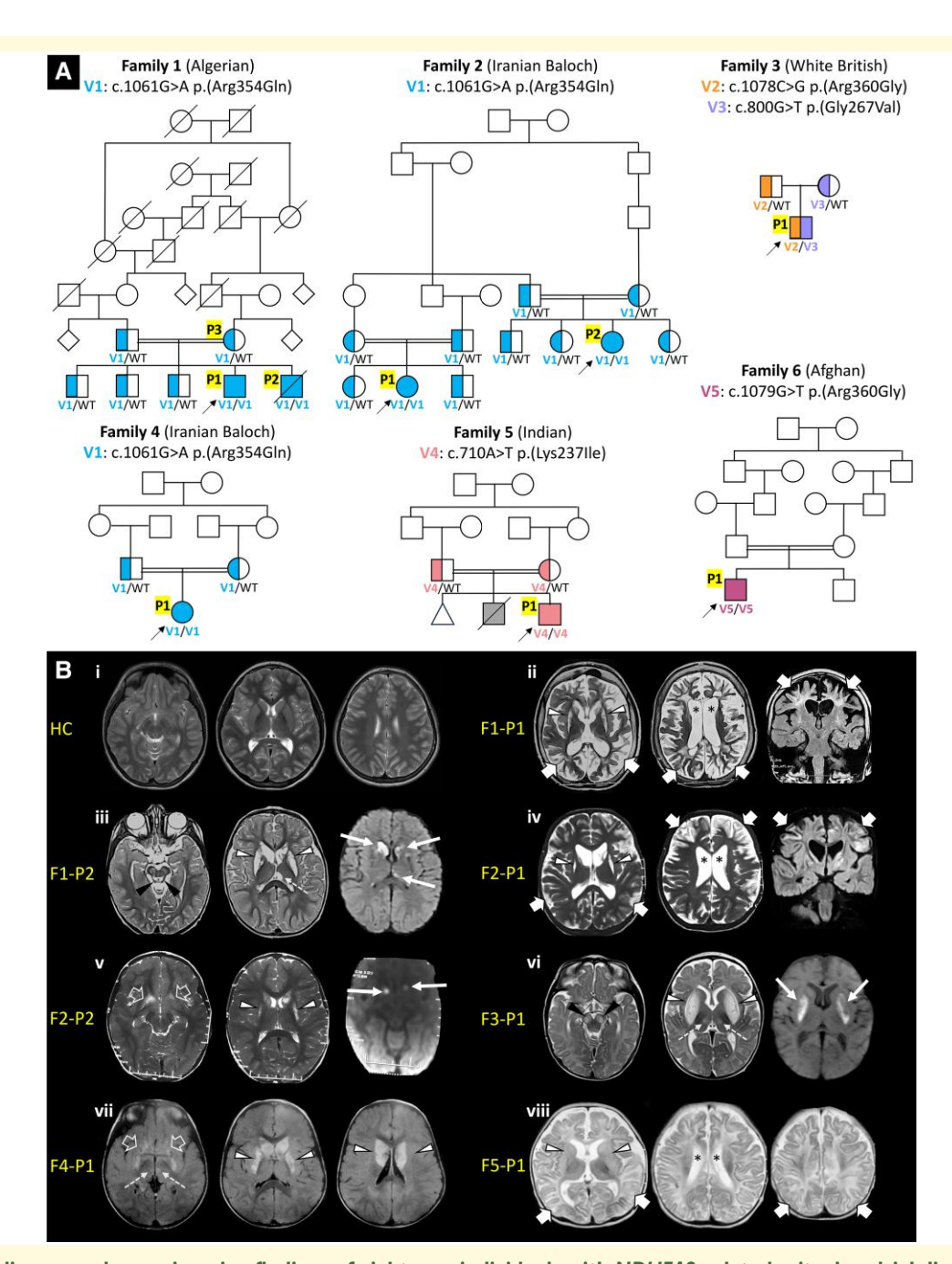


Figure I Pedigrees and neuroimaging findings of eight new individuals with NDUFA9-related mitochondrial disease. (A) Pedigrees of eight new cases of NDUFA9-related mitochondrial disease reported in this study with their ethnicity and results of segregation analysis of NDUFA9 variants. Probands are identified by arrows. Fully filled coloured symbols indicate affected individuals (P#) carrying NDUFA9 variants in the homozygous or compound heterozygous state. Half-filled coloured symbols identify asymptomatic heterozygous carriers of a mutant NDUFA9 allele. Each colour represents a different NDUFA9 variant (V#; see also Fig. 2 and Supplementary File 3). A fully filled grey symbol represents lack of molecular diagnosis in a family member with congenital heart disease. Deceased individuals are identified by a diagonal line. (B) Brain MRI examinations of a healthy control (HC) (i) and of affected individuals FI-PI at 7 years of age (ii), FI-P2 at 4 years (iii), F2-PI at 5 years of age (iv), F2-P2 at 3 years of age (v), F3-P1 at 6 months of age (vi), F4-P1 at 2 years of age (vii), and F5-P1 at 5 months of age (viii). There are bilateral T2 hyperintensities of the putamen and caudate nuclei in all affected individuals (white arrowheads) associated with atrophy in all except three affected individuals (F3-P1, F4-P1 and F5-P1). Focal thalamic signal alterations are present in affected individuals F2-P2, F3-P1 and F4-P1 (white dashed arrows). Involvement of the accumbens nuclei is indicated by white empty arrows. Additional symmetric midbrain T2 hyperintensities (black arrowheads) are depicted in affected individuals FI-P2 and F3-P1. Asymmetric foci of restricted diffusion are present at the level of the basal ganglia (white thin arrows) in individuals F1-P2, F2-P2 and F3-P1. Moderate-to-severe white matter volume loss with enlarged ventricles (black asterisks) are associated with multiple areas of supratentorial cortico-subcortical signal alterations and atrophy (white thick arrows) in patients FI-PI, F2-PI and F5-PI at first MRI. White matter cystic rarefaction is noted in the deep white matter in proband FI-PI and in the subcortical regions in F2-P1. F#, family; HC, healthy control; P#, patient; V#, NDUFA9 variant; WT, wild-type NDUFA9 allele.

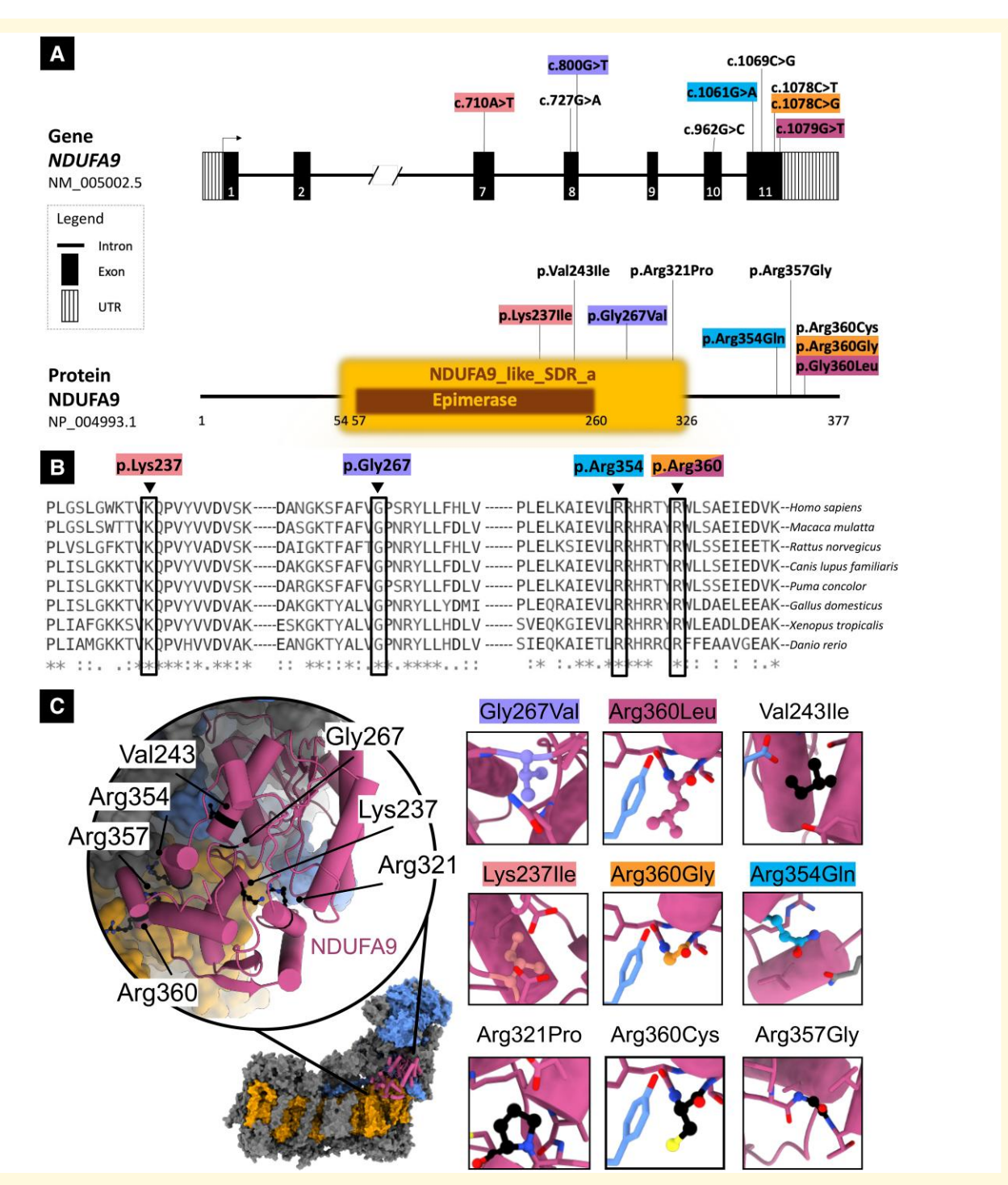


Figure 2 Location, computational analysis and conservation of NDUFA9 variants. (A) Schematic of NDUFA9 and its protein product with five new variants identified in this study and four variants identified in previously reported families. Upper part. Schematic of NDUFA9 with variants identified in this study (coloured; see also Fig. 1A and Supplementary File 3) and previously reported. Introns are not to scale. Exon numbers are according to the canonical transcript (NM_006814.5). Lower part. Schematic of NDUFA9 protein with amino acid changes linked to disease (NP_006805.2). (B) Interspecies alignment showing strong evolutionary conservation of the amino acids affected by the new NDUFA9 missense variants identified in this study across species, down to invertebrates. (C) In silico analysis of human complex I NDUFA9 variants. NDUFA9 (pink) is one of 31 supernumerary subunits (others grey) of mitochondrial complex I that wrap around the core subunits, which compose a membrane arm (orange) and a hydrophilic, matrix arm (blue). The human complex I model (PDB 5XTD) shows how NDUFA9 helps to bind the hydrophilic domain to the membrane through protein—lipid interactions. Inset of NDUFA9 demonstrates the wild-type amino acid locations and conformations (black ball and sticks). Specific mutations of these residues are indicated and a prediction of their rotamer conformation shown (ball and stick), with immediate vicinity residues (within 4 Å) also displayed to highlight disruption to electrostatic interactions (Lys237Ile, Arg321Pro, Arg354Gln, Arg357Gly), lipid binding (Arg360Leu, Arg360Gly, Arg360Cys), as well as increased clashing (Gly267Val, Val243Ile). SDR, short-chain dehydrogenase/reductase; UTR, untranslated region.

Fibroblast preparation, SDS-PAGE and Western blot analysis

Steady-state levels of important complex I subunits and other OXPHOS components were assessed by sodium dodecyl sulfate-polyacrylamide polyacrylamide gel electrophoresis (SDS-PAGE) of study participants and healthy control fibroblast cell lysates as previously described.²¹ Proteins of interest were bound by overnight incubation at 4°C with antibodies against NDUFA9, NADH:ubiquinone oxidoreductase core subunit V1 (NDUFV1), NADH:ubiquinone oxidoreductase subunit B8 (NDUFB8; all complex I), succinate dehydrogenase complex iron sulphur subunit B (SDHB; complex II), ubiquinol-cytochrome c reductase core protein 2 (UOCRC2; complex III), mitochondrially encoded cytochrome c oxidase II (MT-CO2; complex IV), ATP synthase F1 subunit alpha (ATP5A; complex V) and glyceraldehyde-3-phosphate dehydrogenase (GAPDH) as a loading control, followed by horseradish peroxidase (HRP)-conjugated secondary antibodies (Dako Cytomation) and visualized using enhanced chemiluminescence (ECL)-prime (GE Healthcare) and BioRad ChemiDoc MP with Image Lab software.

Mitochondrial preparation and blue native electrophoresis

To assess the assembly of respiratory chain complexes, blue native polyacrylamide gel electrophoresis (BN-PAGE) of enriched mitochondrial preparations solubilized with n-Dodecyl $\beta\text{-D-maltoside}$ from patient-derived fibroblasts and age-matched control cell-lines were performed as previously described. 22

Statistical analysis

Statistics were performed using Microsoft Excel. For descriptive statistics, results are provided as fractions and/or percentages for dichotomous variables and as mean with range for continuous variables. Results of mitochondrial complex I enzymatic activity are reported as means \pm standard deviations (SD).

Results

We identified eight new cases of *NDUFA9*-related mitochondrial disease belonging to six unrelated families of Asian, European and North African ancestry (Fig. 1A). Videos of seven new affected individuals were available (Supplementary Video 1). Pheno-genotypic features of our cohort and four unrelated cases belonging to four families identified through the systematic literature review are detailed in Table 1 and Supplementary File 1.

Phenotypic features

Among eight new and four previously published *NDUFA9* cases, 8/12 (66.7%) were males and 4/12 (33.3%) were

females. Parental consanguinity was reported in all but two affected individuals (10/12, 83.3%; F3-P1, F8-P1). Two of 10 (20%) families had more than one similarly affected member (F1 and F2). Three probands (F3-P1, F7-P1 and F9-P1) died during infancy (range: 1–8 months), and one other affected individual (F1-P2) died at the age of 13 years. In 8/12 (66.7%) affected individuals who were alive at the time of the study or reporting, the age at last assessment ranged from 2.5 years to mid-40s.

Three of 12 (25.0%) individuals were born preterm. Delivery via caesarean section was reported in 1/12 (8.3%) case. Perinatal issues were described in 5/12 (41.7%) affected individuals, including respiratory distress/insufficiency (three cases), hypotonia (two cases) and bradycardia (one case). Neurodevelopmental delay followed by motor deterioration and seizures were the most common presenting features. Among 10/12 (83.3%) cases who survived beyond the age of 4 months, motor and/or speech and language developmental delay was observed in nine (90.0%). Among 9/12 (75.0%) cases who survived beyond infancy, five (55.5%) individuals never attained unsupported sitting, and six (66.7%) cases were reported with moderate-tosevere intellectual disability. Onset of neurological deterioration invariably occurred within the first decade of life (range: neonatal period—9 years) and prior to age the age of 4 years in 9/12 (75.0%) cases. When neurological deterioration began, worsening of motor performance or motor regression was reported as the earliest manifestation in 8/ 12 (66.7%) cases and seizures in 3/12 (25.0%).

Among 10/12 (83.3%) cases surviving beyond the age of 4 months, main clinical manifestations encompassed dystonia (10/10, 100%), feeding difficulties/dysphagia/failure to thrive and pyramidal tract signs (8/10, 80%), seizures and muscle weakness/atrophy (7/10, 70%), and dysarthria/anarthria/stuttering (6/10, 60%). Dystonia was generalized since onset in 7/10 cases (70%), whereas it started in the distal lower limbs and progressed to a generalized form in 2/10 cases (20%) and remained multifocal in 1/10 case (10%). Of seven individuals with seizures, five (71.4%) experienced only generalized seizures, and two (28.6%) had both focal motor and generalized seizures. Seizures were of tonic type in most cases, and status epilepticus was reported in one case 1/7 case (14.3%) during a respiratory infection (Table 1 and Supplementary File 1).

Minor phenotypic features include strabismus (3/10, 30%), scoliosis (2/10, 20%), ataxia (2/10, 20%), and peripheral sensorimotor neuropathy (1/10, 10%). In three cases who died during infancy, one had retinopathy of prematurity, one had retinitis pigmentosa, and one had hearing loss. Additional clinical information is detailed in Table 1 and Supplementary File 1.

Among cases with biochemical tests available, blood lactate was increased in 8/9 (88.9%) where available, and CSF lactate was raised in 2/5 (40.0%) where available. Five affected individuals underwent respiratory chain enzyme testing in dermal fibroblasts and/or muscle tissue, with confirmation of isolated complex I deficiency in all

Table | Summary of clinical, neuroradiological and genetic features of new and previously reported cases of NDUFA9-related mitochondrial disease

`				•							
<u>.</u>		7		E		Æ	F6	F7	F 8	F9	FI0
PI P2 PI	_		P2	I.	<u>-</u>	۵	Ы	Ы	F	۵	F
Σ	ш		ш	Σ		Σ	Σ	Σ	Σ	Σ	ш
18 mo 26 mo 4 yr	4 yr		8 yr	7 mo		3 mo	2.5 yr	Neonatal	7 yr	Neonatal	9 yr
19 yr (†) 8 yr	8 yr		12 yr	8 mo (†)		33 mo	I5 yr	I mo (†)	Mid-40s	4 mo (†)	26 yr
Algerian Algerian Iranian	anian		Iranian	White British		Indian	Afghan	Iraqi	Chinese	Iranian	Indian
>	>		>	z		>	>	≻	z	>	>
>	>		>	z		~٠	z	z	z	z	z
z ≻	z		z	>		z	z	>	z	>	z
>	≻		>	> -		>	>	∢ Z	z	>	z
, , ,	>		z	>		∢ Z	>	∢ Z	z	z	z
Y (mod) Y (mod) Y (sev)	(sev)		Y (mod)	∀ /Z		Y (sev)	∢ Z	∢ Z	z	ΥZ	z
\ \ \ \ \ \ \ \ \ \ \ \ \ \ \ \ \ \ \	>		>	>		<u>·</u>	>	>	>	z	>
\ \ \	>		>	Y/Z		>	>	∢ Z	>	>	z
\ \ \	>		> -	>		>	>	∢ Z	z	>	z
\ \ \	>		>	∀ /Z		∢ Z	z	∢ Z	>	ΥZ	z
> > >	>		>	z		>	>	z	z	>	z
\ \	>		>	>		>	>	z	z	z	z
>	>		>	>		>	>	>	>	>	>
Y (bl) Y (bl) Y (bl)			A/N	Y (bl, CSF)		Y (bl)	∢ Z	Y (bl, ur)	Y (bl)	Y (bl, CSF)	z
Hom Hom Hom	_		Hom	C-Het		Hom	Hom	Hom	Hom	Hom	Hom
c.1061G > A c.1061G > A c.1061G > A c.	۸ ۸		1061G > A	c.1078C > G		c.710A > T	:.1079G > T	c.962G > C	c.1078C > T	c. 1069C > G	2.727G > A
p.(R354Q) p.(R354Q) p.(R354Q)	ô).(R354Q)	p.(R360G) &	p.(R354Q)	p.(K237I)	p.(R360L)	p.(R321P)	p.(R360C)	p.(R357G)	p.(V243I)
				c.800G > T							
: :			-	p.(G267V)	i	i	i	71 41	<u>v</u>	4	17
This article This article This article	sarticle		l his article	This article	I his article	I his article	I his article		2	2	

See also Fig. I A and Supplementary File I. bl, blood; C-Het, compound heterozygote; F, female; F#, family; FTT, failure to thrive; Het, heterozygote; Hom, homozygote; ID, intellectual disability; M, male; mo, month(s); mod, moderate; N, no (absent); N/A, not applicable/not available; NDD, neurodevelopmental delay; P#, patient; sev, severe; ur, urine; Y, yes (present); yr, year(s); †, age at death.

and detection of a complex I stalled assembly intermediate in one individual (F3-P1).

Brain MRI examinations were available for review in all eight new affected individuals. MRI scans were performed at a mean age of 3.1 years (range: 5 months-7 years). All individuals showed bilateral symmetric or asymmetric signal alterations of the basal ganglia (8/8, 100%) with associated mild-to-severe atrophy in four cases (50.0%) and swelling in two individuals (25.0%; Fig. 1B). In particular, the putamen and caudate nuclei were involved in 8/8 cases (100%), the accumbens nuclei in 5/8 (62.5%), the thalami in 3/8 (37.5%) and the globi pallidi in 3/8 individuals (37.5%). Diffusion weighted images (DWI) were available in three cases, showing foci of restricted diffusion in all individuals at the level of the putamina (n = 2; 66.7%), caudate nuclei (n = 1; 33.3%), accumbens nuclei (n = 1; 33.3%), and thalamus (n = 1;33.3%). In 4/8 individuals (50.0%), there was moderate-tosevere white matter volume loss and signal alterations, with thin corpus callosum and enlarged ventricles; in three of these individuals, there were also multiple regions of cortical-subcortical signal alterations and atrophy associated with white matter cavitations (n = 2 in the deep white matter and n = 1 in the subcortical white matter); these findings were consistent with a leukodystrophy with cystic rarefaction associated with multifocal cortical atrophy. Finally, in 3/8 individuals, bilateral symmetric signal alterations were noted in the brainstem, including the central tegmental tracts and cerebral peduncles (n = 3), periaqueductal gray matter (n=2), and posterior medulla (n=1). In two individuals (F1-P1 and F1-P2), follow-up brain MRI performed at the age of 17 and 12 years, respectively showed marked progression of the cerebral and basal ganglia atrophy associated significant worsening of the leukodystrophy (Supplementary File 2). Brain MR spectroscopy did not show lactate or other metabolite peak in two cases where available.

EEG showed multifocal epileptic activity or was normal at different stages in individuals with history of seizures (Supplementary File 1). Ophthalmological assessment was performed in two affected individuals who survived into the second decade of life; one individual showed bilateral papillary pallor, while the other had normal findings. Visual evoked potentials were normal in two probands where performed. EMG/NCS was performed in three affected individuals, showing axonal sensorimotor neuropathy in one and being normal in two.

Genetic findings

We identified five new missense variants in *NDUFA9* (ENST00000266544.10; NM_005002.5; NP_006805.2; Fig. 2A), thereby expanding the known genotypic spectrum of *NDUFA9*-related mitochondrial disorder. Previously, only four missense variants had been reported [c.962G > C p.(Arg321Pro), c.1078C > T p.(Arg360Cys), c.1069C > G p.(Arg357Gly), c.727G > A p.(Val243Ile)]. Among the newly identified *NDUFA9* variants, one variant recurred in three

unrelated pedigrees [c.1061G > A p.(Arg354Gln), F1-F2-F4], and two variants were detected in two unrelated pedigrees [c.1078C > G p.(Arg360Gly), F3; c.1079G > T p.(Arg360Leu), F6] and affected the same nucleotide of another previously reported variant [c.1078C>T p.(Arg360Cys), F8], which therefore emerges as a possible mutational hotspot (Fig. 2A). 15 In all new cases with genomic DNA available, segregation analysis revealed that biallelic NDUFA9 variants co-segregated with neurological disease phenotypes, whereas unaffected parents and siblings of affected individuals harboured one heterozygous NDUFA9 variant (Fig. 1A). Among eight new affected individuals, seven were homozygotes and one compound heterozygote for NDUFA9 variants (Fig. 1A). Variants analysis is detailed in Supplementary File 3. All NDUFA9 variants identified in this study were not observed in the homozygous state or ultra-rare in the heterozygous state in gnomAD v4.1.0, other open-source population databases and private nextgeneration sequencing repositories (Supplementary File 3). NDUFA9 variants identified in this study showed strong evolutionarily conservation across species down to invertebrates (Fig. 2B). All NDUFA9 variants were predicted with a damaging effect according to most in silico prediction tools (Supplementary File 3). All NDUFA9 variants had a high CADD Phred score (range: 23.6-33) and REVEL score ranging from 0.27 to 0.94. Pathogenicity prediction tools such as PolyPhen-2, SIFT 4G and MutationTaster predicted the functional impact of all NDUFA9 missense variants to be damaging/deleterious in most cases (Supplementary File 3). According to the ACMG/AMP guidelines, NDUFA9 variants identified in new cases were classified as pathogenic [c.800G > T p.(Gly267Val)], likely pathogenic [c.1061G > A p.(Arg354Gln); c.1078C > G p.(Arg360Gly) and variant of uncertain significance [c.710A > T p.(Lys237Ile); c.1079G > T p.(Arg360Leu)]. No additional biallelic variants of (likely) pathogenic significance were identified in the affected individuals.

Potential effects of the variants to NDUFA9 folding and binding

NDUFA9 variants can introduce disruption to electrostatic and packing interactions, which can lead to protein misfolding and/or disruption to binding interfaces. Among nine new and previously reported variants in NDUFA9, six replace Arginine with Leucine, Glycine, Glutamine, Cysteine or Proline residues, and one is a Lysine to Isoleucine. All substitutions remove the positive charge and affect stability of negative amino acids in structurally important ion pairs (Fig. 2C, Lys237Ile and Arg321Pro). Additionally, Arginine has important interactions with negatively charged phospholipid headgroups when located on membranebinding surface, such as Arg360, where they help to embed the subunit and anchor the hydrophilic domain of complex I. Arg360Leu, Arg360Gly and Arg360Cys will all disrupt this capacity. The two variants that do not affect the electrostatics, Gly267Val and Val243Ile, both have detrimental impact by introducing unfavourable clashing interactions due to their larger size, particularly Gly267Val.

Western blot and biochemical analysis of fibroblasts

To further investigate the effect of three NDUFA9 variants identified in this study on mitochondrial function, we established dermal fibroblast cultures from skin biopsies obtained from two probands (F1-P1, F3-P1), one affected brother (F1-P2) of proband F1-P1 and their asymptomatic mother (F1-P3). SDS-PAGE immunoblotting using antibodies against various structural subunits of complex I revealed an overall reduction in the steady-state levels of NDUFA9 protein in the cells from affected individuals F1-P1 and F1-P2 compared to healthy controls (Fig. 3A; Supplementary File 4), whilst normal levels were detected in cells from F3-P1 and F1-P3. Levels of key subunits of complex II, complex III, complex IV and complex V were all normal (Fig. 3A). Immunoblotting using antibodies conjugated against structural subunits from all OXPHOS complexes showed a loss of fully assembled complex I in cells from F3-P1, F1-P1 and F1-P2, while all other OXPHOS complexes were unaffected (Fig. 3B; Supplementary File 4). Furthermore, analysis of F3-P1 cells appeared to show the presence of a partially assembled, smaller complex I intermediate (Fig. 3B; Supplementary File 4). Cells from F1-P3 revealed a profile indistinguishable from healthy controls. Assessment of mitochondrial respiratory chain enzyme activities revealed isolated complex I deficiency in the fibroblasts from F1-P1 (complex I activity: 0.133 nmols NADH oxidized.min⁻¹.unit citrate synthase⁻¹) and F3-P1 (0.114 nmols NADH oxidized.min⁻¹.unit citrate synthase⁻¹), although surprisingly fibroblasts from F1-P2 showed normal complex I activity (0.197 nmols NADH oxidized.min⁻¹.unit citrate synthase⁻¹; controls 0.197 ± 0.034 [mean \pm SD, n = 8]); all other respiratory chain complex activities were normal. As expected, no mitochondrial biochemical abnormalities were detected in the fibroblasts from F1-P3 (complex I activity: 0.244 nmols NADH oxidized.min⁻¹.unit citrate synthase⁻¹).

Discussion

Isolated complex I deficiency is the most frequent childhood-onset OXPHOS disorder. ¹¹⁻¹³ Most cases present with neurodevelopmental delay and progressive neurological deterioration with clinical manifestations of basal ganglia and/or brainstem dysfunction, elevated blood or CSF lactate, and MRI or pathological evidence of basal ganglia and/or brainstem abnormalities, which leads to the diagnosis of LS. ¹² Presentations not fulfilling all the above-mentioned criteria are labelled as Leigh-like syndrome (LLS). Taken together, disease-causing variants in genes encoding complex I subunits represent the major cause of LS/LLS. However, information on the pheno-genotypic spectrum linked to defects in most individual complex I subunits is scarce.

With the present study, 12 NDUFA9 cases from 10 families have been reported. NDUFA9-related mitochondrial disease shows wide phenotypic variability, with clinical presentation ranging from typical LS with lethality during the neonatal period to childhood-onset, isolated, generalized dystonia with survival into adulthood. 14-17 Notably, neurological deterioration always started within the first decade of life and was triggered by infections/febrile episodes in few cases. Most NDUFA9 patients showed neurodevelopmental delay/intellectual disability and complex movement abnormalities, in keeping with the phenotypic spectrum reported for other mitochondrial disorders caused by mutations in nuclear and mitochondrial DNA genes encoding complex I subunits.²³ In NDUFA9-related mitochondrial disease, dystonia was the most prominent motor features, followed by pyramidal tract signs.^{23,24} As recently reviewed by members of our team, ²³ prominent dystonia, most often in the context of a neurodevelopmental disorder, is a common presentation in cases of NDUFS6-, NDUFAF5-, NDUFS7-, NDUFA12-, 24 NDUFS1-, NDUFS4-, MT-ND1-, and MT-ND3-related mitochondrial disease. Over two thirds of NDUFA9 cases had a history of seizures, which had not been reported in previously published NDUFA9 cases and was however not infrequent in cases of NDUFS4-, NDUFS8-, NDUFV1-, NDUFAF5-, NUBPL-, MT-ND1-, MT-ND3-, MT-ND5-, and MT-ND6-related mitochondrial disease.²³ Increased blood lactate levels were the most common albeit inconstant biochemical finding. When available, brain MRI always revealed a LS pattern characterized by bilateral, mostly symmetric basal ganglia signal alterations associated with atrophy or swelling and additional foci of restricted diffusion. Similar neuroradiological findings were previously described in three individuals harbouring biallelic NDUFA9 variants, 14,15,17 which suggests a selective vulnerability of these anatomical structures. In addition, in two individuals we found other typical neuroimaging manifestations of LS, with bilateral and symmetric periaqueductal gray matter, cerebral peduncles, central tegmental tracts and posterior medulla signal alterations.²⁵ Four patients had white matter signal alterations and volume loss, in keeping with a leukodystrophy with additional cystic rarefaction in three cases.²⁶ Of note, in two subjects, the cysts were large and located in the deep white matter, as previously described in other mitochondrial disorders. 26 Conversely, in one case, the cystic rarefaction was subtle and located in the subcortical regions, an atypical finding in mitochondrial leukodystrophies.²⁶ Interestingly, the previously unreported association of a cavitating leukodystrophy with early and prominent cortical atrophy expands the neuroimaging phenotype of NDUFA9related disease.

From a genotypic perspective, all nine *NDUFA9* variants linked to human disease so far are missense mutations, which might suggest that complete loss of function is not compatible with complex I assembly and/or functioning and ultimately with survival in humans. Intriguingly, none of the NDUFA9 variants hitherto reported maps at the N-terminal of the protein, where the presequence addressing

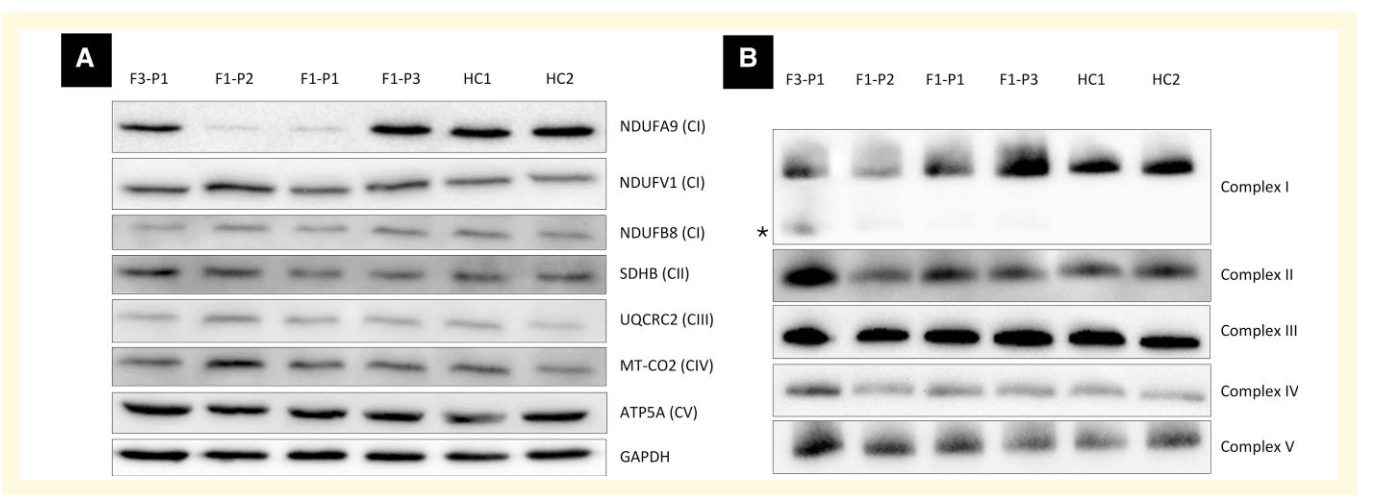


Figure 3 Western blot and biochemical assessment of Iysates from dermal fibroblasts of individuals with biallelic NDUFA9 variants. (A) Whole-cell (fibroblast) Iysates from individuals F3-P1 (affected), F1-P2 (affected), F1-P3 (unaffected carrier; Fig. IA) and age-matched healthy controls (HC1, HC2) were analysed by SDS-PAGE. Immunoblotting was performed with antibodies against complex I subunits and several OXPHOS subunits as indicated, with GAPDH (cytosolic protein) utilized as a loading control. C# indicates mitochondrial complexes I to V. (B) Mitochondria isolated from cultured dermal fibroblasts from individuals F3-P1 (affected), F1-P2 (affected), F1-P1 (affected), F1-P3 (unaffected carrier; Fig. IA) and age-matched healthy controls (HC1, HC2) were solubilized in n-dodecyl β-D-maltoside (DDM) and subjected to BN-PAGE and immunoblotting analysis using antibodies directed to various OXPHOS complexes, NDUFB8 (CI), SDHA (CII), UQCRC2 (CIII), MT-CO2 (CIV), ATP5A (CV). The blot probed with an antibody raised against NDUFB8 (CI) revealed the presence of an additional partially assembled complex I intermediate in proband F3-P1 (asterisk). ATP5A, ATP synthase F1 subunit alpha; BN-PAGE, blue native polyacrylamide gel electrophoresis; CI, complex I; CII, complex II; CIII, complex III; CIV, complex IV; CV, complex V; F#, family; GAPDH, glyceraldehyde-3-phosphate dehydrogenase; HC#, healthy control; MT-CO2, mitochondrially encoded cytochrome c oxidase II; NDUFA9, NADH:ubiquinone oxidoreductase subunit A9; NDUFV1, NADH:ubiquinone oxidoreductase core subunit V1; NDUFB8, NADH:ubiquinone oxidoreductase subunit B8; SDHB, succinate dehydrogenase complex iron sulphur subunit B; P#, patient; UQCRC2, ubiquinol-cytochrome c reductase core protein 2. Full-size and uncropped blots/gels are presented in Supplementary File 4.

the synthetized protein to mitochondria is located. On the contrary, most variants identified in human *NDUFA9* cases lie in the last exon, including three variants affecting the residue Arg360, which we herein highlight as a possible mutational hotspot.

NDUFA9 sits at the interface of the membrane and matrix arms of mitochondrial complex I and plays a role in securing the hydrophilic domain to the membrane. This is achieved by the binding of negative phospholipids to largely positively charged amino acids (e.g. Lysine and Arginine) found on NDUFA9 membrane-interacting face. In this study, protein modelling revealed that NDUFA9 missense variants hitherto reported are implicated in protein misfolding through clashing or unfavourable electrostatic interactions. Notably, six NDUFA9 variants affect wild-type Arginine residues. Arginine has an important role in anchoring the NDUFA9 subunit and stabilizing the enzyme through binding and remodelling the phospholipid bilayer. NDUFA9 amino acid changes affecting these residues could interfere with the recruitment of the membrane-bound substrate ubiquinone-10 and ultimately disrupt complex I function.^{7,8}

Our experiments investigating mitochondrial function in fibroblasts from three new *NDUFA9* cases invariably showed loss of fully assembled complex I. Furthermore, decreased steady-state levels of NDUFA9 protein were detected in two related homozygotes for the variant Arg354Gln. On

the contrary, levels observed in one compound heterozygote for the variants c.1078C > G p.(Arg360Gly) and c.800G > T p.(Gly267Val) were similar to healthy controls. Intriguingly, the same affected individual showed a partially assembled, smaller complex I intermediate. This observation parallels *in vitro* evidence that NDUFA9 contributes to stability of a later stage complex I assembly in *NDUFA9* knockout in HEK293T cells from a previous study.⁶

In conclusion, our study provides further evidence of the pheno-genotypic spectrum associated with biallelic *NDUFA9* variants and mitochondrial complex I deficiency. This evidence supports the inclusion of *NDUFA9* variants in the diagnostic workup of complex movement disorders encompassing dystonia and/or pyramidal features and a LS pattern of brain MRI signal abnormalities. Future case reporting may expand our understanding of *NDUFA9*-related mitochondrial disease and help establish whether genotype-phenotype correlations exist. To date, such correlations have been hampered by the limited number of reported cases and variants, most of which are private.

Supplementary material

Supplementary material is available at *Brain Communications* online.

Acknowledgements

The Authors are grateful to patients who participated in this study and their families. Molecular graphics and analyses were performed with UCSF ChimeraX, developed by the Resource for Biocomputing, Visualization, and Informatics at the University of California, San Francisco, with support from National Institutes of Health R01-GM129325 and the Office of Cyber Infrastructure and Computational Biology, National Institute of Allergy and Infectious Diseases.

Funding

There is no specific funding relevant to this work. F.M. was supported by the Edmond J. Safra Clinical Research Fellowship in Movement Disorders and acknowledges current funding through the National Institute for Health and Care Research (NIHR) University College London Hospitals (UCLH) Research Centre (BRC) Translational Biomedical Neuroscience Intermediate Clinical Fellowship (Grant ID: BRC1287/TN/FM/101410), the Edmond J. Safra Movement Disorders Research Career Development Award (Grant ID: MJFF-023893), Parkinson's UK (Grant ID: G-2401), the American Parkinson Disease Association (Grant ID: 1282403) and the David Pearlman Charitable Foundation. D.N.G. is funded by the grants MC UU 00015/2 and MC UU 00028/1. C.L.A. is supported by the National Institute for Health Research (NIHR) Post-Doctoral Fellowship (PDF-2018-11-ST2-021). The views expressed in this publication are those of the author(s) and not necessarily those of the National Health Service (NHS), the National Institute for Health and Care Research (NIHR), or the Department of Health and Social Care. Kailash P. Bhatia receives royalties from publication of the Oxford Specialist Handbook Parkinson's Disease and Other Movement Disorders (Oxford University Press, 2008), of Marsden's Book of Movement Disorders (Oxford University Press, 2012), and of Case Studies in Movement Disorders-Common and uncommon presentations (Cambridge University Press, 2017). He has received honoraria/personal compensation for participating as consultant/scientific board member from Ipsen, Allergan, Merz and honoraria for speaking at meetings and from Allergan, Ipsen, Merz, Sun Pharma, Teva, UCB Pharmaceuticals and from the American Academy of Neurology and the International Parkinson's Disease and Movement Disorders Society. R.W.T. is funded by the Wellcome Centre for Mitochondrial Research (203105/Z/16/ Z), the Mitochondrial Disease Patient Cohort (UK) (G0800674), the Medical Research Council (MR/W019027/ 1), the Lily Foundation, the Pathological Society, the UK National Institute for Health and Care Research (NIHR) Biomedical Research Centre (BRC) for Aging and Age-related disease award to the Newcastle upon Tyne Foundation Hospitals National Health Service (NHS) Trust, LifeArc and the UK National Health Service (NHS) Highly Specialised Service for Rare Mitochondrial Disorders of Adults and

Children. Henry Houlden and the Houlden lab are grateful for the important support from UK and international collaborators, brain banks and biobanks, and grateful for essential funding from Wellcome Trust, Medical Research Council (MRC), Multiple System Atrophy (MSA) Trust, National Institute for Health Research (NIHR) University College London Hospitals (UCLH) Biomedical Research Centre (BRC), Michael I. Fox Foundation (MIFF), Fidelity Trust, Rosetrees Trust, Dolby Family fund, Alzheimer's Research UK (ARUK), Multiple System Atrophy (MSA) Coalition, Parkinson's UK, Parkinson's Foundation, The Guarantors of Brain, Cerebral Palsy Alliance, Friedreich's Ataxia Research Alliance (FARA), European Academy of Neurology (EAN), Victorian Brain Bank, the National Institutes of Health (NIH) NeuroBioBank, Queen Square Brain Bank, The Medical Research Council (MRC) Brain Bank Network.

Competing interests

The authors report no competing interests relevant to this work.

Data availability

The authors confirm that the data supporting the findings of this study are available within the article, its supplementary material and from the corresponding authors, upon reasonable request. No code was generated or used for this study.

References

- Vercellino I, Sazanov LA. The assembly, regulation and function of the mitochondrial respiratory chain. Nat Rev Mol Cell Biol. 2022; 23(2):141-161.
- Kampjut D, Sazanov LA. Structure of respiratory complex I—An emerging blueprint for the mechanism. Curr Opin Struct Biol. 2022;74:102350.
- Parey K, Wirth C, Vonck J, Zickermann V. Respiratory complex I— Structure, mechanism and evolution. Curr Opin Struct Biol. 2020; 63:1-9.
- Vinothkumar KR, Zhu J, Hirst J. Architecture of mammalian respiratory complex I. Nature. 2014;515(7525):80-84.
- Balsa E, Marco R, Perales-Clemente E, et al. NDUFA4 is a subunit of complex IV of the mammalian electron transport chain. Cell Metab. 2012;16(3):378-386.
- Stroud DA, Formosa LE, Wijeyeratne XW, Nguyen TN, Ryan MT. Gene knockout using transcription activator-like effector nucleases (TALENs) reveals that human NDUFA9 protein is essential for stabilizing the junction between membrane and matrix arms of complex I. J Biol Chem. 2013;288(3):1685-1690.
- Parey K, Haapanen O, Sharma V, et al. High-resolution cryo-EM structures of respiratory complex I: Mechanism, assembly, and disease. Sci Adv. 2019;5(12):eaax9484.
- Gu J, Liu T, Guo R, Zhang L, Yang M. The coupling mechanism of mammalian mitochondrial complex I. *Nat Struct Mol Biol.* 2022; 29(2):172-182.
- Grba DN, Wright JJ, Yin Z, Fisher W, Hirst J. Molecular mechanism of the ischemia-induced regulatory switch in mammalian complex I. *Science*. 2024;384(6701):1247-1253.

- McCormick EM, Keller K, Taylor JP, et al. Expert panel curation of 113 primary mitochondrial disease genes for the Leigh syndrome spectrum. Ann Neurol. 2023;94(4):696-712.
- 11. Distelmaier F, Koopman WJ, van den Heuvel LP, *et al.* Mitochondrial complex I deficiency: From organelle dysfunction to clinical disease. *Brain.* 2009;132(Pt 4):833-842.
- 12. Lake NJ, Compton AG, Rahman S, Thorburn DR. Leigh syndrome: One disorder, more than 75 monogenic causes. *Ann Neurol*. 2016; 79(2):190-203.
- 13. Schubert Baldo M, Vilarinho L. Molecular basis of Leigh syndrome: A current look. *Orphanet J Rare Dis.* 2020;15:31.
- 14. van den Bosch BJ, Gerards M, Sluiter W, *et al.* Defective NDUFA9 as a novel cause of neonatally fatal complex I disease. *J Med Genet*. 2012;49(1):10-15.
- Baertling F, Sánchez-Caballero L, van den Brand MAM, et al. NDUFA9 point mutations cause a variable mitochondrial complex I assembly defect. Clin Genet. 2018;93(1):111-118.
- 16. Gholamipour Shirazi P, Heidari A, Farshadmoghadam H. Novel missense variation in NDUFA9 gene in an Iranian patient with fatal Leigh syndrome. *Iran J Pediatr*. 2022;32(3):e115845.
- Singh R, Padmanabha H, Arunachal G, Mailankody P, Mahale RR. Childhood-onset generalized dystonia due to NDUFA9 gene mutation: An expansion of mutations causing Leigh's syndrome. *Ann Indian Acad Neurol*. 2023;26(4):606-608.
- 18. Richards S, Aziz N, Bale S, et al. Standards and guidelines for the interpretation of sequence variants: A joint consensus recommendation of the American College of Medical Genetics and Genomics

- and the Association for Molecular Pathology. *Genet Med.* 2015; 17(5):405-424.
- Guo R, Zong S, Wu M, Gu J, Yang M. Architecture of human mitochondrial respiratory megacomplex I₂III₂IV₂. Cell. 2017;170(6): 1247-1257.e12.
- Meng EC, Goddard TD, Pettersen EF, et al. UCSF ChimeraX: Tools for structure building and analysis. Protein Sci. 2023;32(11):e4792.
- Thompson K, Majd H, Dallabona C, et al. Recurrent De Novo dominant mutations in SLC25A4 cause severe early-onset mitochondrial disease and loss of mitochondrial DNA copy number. Am J Hum Genet. 2016;99(6):1405.
- 22. Oláhová M, Hardy SA, Hall J, et al. LRPPRC mutations cause early-onset multisystem mitochondrial disease outside of the French-Canadian population. *Brain*. 2015;138(Pt 12):3503-3519.
- 23. Kaiyrzhanov R, Thompson K, Efthymiou S, *et al.* Biallelic NDUFA13 variants lead to a neurodevelopmental phenotype with gradual neurological impairment. *Brain Commun.* 2024;7(1):fcae453.
- 24. Magrinelli F, Cali E, Braga VL, *et al.* Biallelic loss-of-function NDUFA12 variants cause a wide phenotypic spectrum from Leigh/Leigh-like syndrome to isolated optic atrophy. *Mov Disord Clin Pract.* 2022;9(2):218-228.
- 25. Bonfante E, Koenig MK, Adejumo RB, Perinjelil V, Riascos RF. The neuroimaging of Leigh syndrome: Case series and review of the literature. *Pediatr Radiol*. 2016;46(4):443-451.
- Roosendaal SD, van de Brug T, Alves CAPF, et al. Imaging patterns characterizing mitochondrial leukodystrophies. AJNR Am J Neuroradiol. 2021;42(7):1334-1340.